Jonathan S. Morrell · Mark J. Jackson
Editors

Uranium Processing and Properties

Springer

Uranium Processing and Properties

Jonathan S. Morrell • Mark J. Jackson
Editors

Uranium Processing and Properties

Springer

Editors
Jonathan S. Morrell
Compatibility and Surveillance Section
Y-12 National Security Complex
Oak Ridge, TN
USA

Mark J. Jackson
Center for Advanced Manufacturing
Purdue University
West Lafayette, IN
USA

ISBN 978-1-4614-7590-3 ISBN 978-1-4614-7591-0 (eBook)
DOI 10.1007/978-1-4614-7591-0
Springer New York Heidelberg Dordrecht London

Library of Congress Control Number: 2013943696

Printed on acid-free paper

Springer is part of Springer Science+Business Media (www.springer.com)

Preface

The processing and properties of uranium and its alloys are the subject of much scrutiny at the present time owing to a resurgence of activity in the field of nuclear technology. This book is a summary of work prepared by experts in the field of uranium, with some special submissions based on presentations and papers included at the "Processing of Specialty Metals with Emphasis on Depleted Uranium Users' Conferences" that were sponsored by the American Society of Materials, Manufacturing Sciences Corporation, and the Y-12 National Security Complex at Oak Ridge, Tennessee. These conferences occurred in 2004, 2007, and 2010 with contributors from academia, industry, and government including the Department of Energy—National Nuclear Security Administration laboratories and facilities, and the Atomic Weapons Establishment at Aldermaston, United Kingdom. The chapters provide an authoritative text on the current developments in the field of processing and properties of uranium.

Chapter 1 focuses on the physical, chemical, mechanical, and metallurgical properties of uranium metal; Chap. 2 focuses on several casting and melting techniques; Chaps. 3 and 4 cover machining with coated cutting tools and the grinding parameters of uranium, respectively; Chap. 5 deals with aqueous extraction techniques and processes with emphasis on the chemical principles involved; Chaps. 6 and 7 focus on uranium corrosion with specific detail on the phase relationships and kinetic processes describing the pure uranium–hydrogen binary system and the ternary processes involving oxygen, respectively; Chap. 8 focuses on the fundamentals supporting nondestructive evaluation techniques as well as the methods themselves which are applicable to uranium systems; lastly, Chap. 9 covers developments of new medical isotope production using low-enriched uranium fuel.

The structure of the book is based on the materials provided by many colleagues, and the author wishes to thank the contributors of this book for helping construct a current source of knowledge and information on uranium processing

and properties as well as for granting the editors permission to use such material. The editors also acknowledge the help and support of Merry Stuber and her colleagues at Springer publishers for help in preparing the manuscript in a timely manner.

Oak Ridge, TN, USA Jonathan S. Morrell
West Lafayette, IN, USA Mark J. Jackson

Contents

Contributors

Rahul Bhola Department of Metallurgical and Materials Engineering, Colorado School of Mines, Golden, CO, USA

Kenneth H. Eckelmeyer 6 Valley View Court, Placitas, NM, USA

Srisharan G. Govindarajan Mechanical and Aerospace Engineering, University of Missouri-Columbia, Columbia, MO, USA

Nathan R. Gubel Department of Metallurgical and Materials Engineering, Colorado School of Mines, Golden, CO, USA

Rodney G. Handy Department of Engineering Technology & Construction Management, University of North Carolina-Charlotte, Charlotte, NC, USA

Cameron Howard Department of Metallurgical and Materials Engineering, Colorado School of Mines, Golden, CO, USA

Mark J. Jackson Center for Advanced Manufacturing, Purdue University, West Lafayette, IN, USA

Kimberly N. Johnson University of Tennessee, Knoxville, TN, USA

Kamalu Koenig Structural Integrity Associates, Inc., Centennial, CO, USA

Brajendra Mishra Department of Metallurgical and Materials Engineering, Colorado School of Mines, Golden, CO, USA

Jonathan S. Morrell Y-12 National Security Complex, Oak Ridge, TN, USA

David L. Olson Department of Metallurgical and Materials Engineering, Colorado School of Mines, Golden, CO, USA

Jonathan Poncelow Department of Metallurgical and Materials Engineering, Colorado School of Mines, Golden, CO, USA

G. Louis Powell Y-12 National Security Complex, Oak Ridge, TN, USA

Edward B. Ripley Y-12 National Security Complex, Oak Ridge, TN, USA

Grant M. Robinson Center for Advanced Manufacturing, Purdue University, West Lafayette, IN, USA

Gary L. Solbrekken Mechanical and Aerospace Engineering, University of Missouri-Columbia, Columbia, MO, USA

Kyler K. Turner Mechanical and Aerospace Engineering, University of Missouri-Columbia, Columbia, MO, USA

Craig VanHorn URS Corporation, Denver, CO, USA

Michael D. Whitfield Center for Advanced Manufacturing, Purdue University, West Lafayette, IN, USA

Chapter 1
Introduction to Uranium

Nathan R. Gubel, Kenneth H. Eckelmeyer, Kimberly N. Johnson, Mark J. Jackson, and Jonathan S. Morrell

Abstract Historical studies of uranium were attributed to its distinction as the heaviest element in nature and as the terminus of the classical periodic table. Presently, the mechanical, physical, chemical, and metallurgical properties of uranium metal are of great importance in nuclear fuels, in weapons, and as a precursor to uranium oxide fuel. New reactor designs, including metal-fueled fast reactors, require the continued research and understanding of uranium material science. All actinide metals exhibit unusual physical properties, as such; the mechanical properties of uranium are highly dependent upon fabrication and heat treatment history as well as impurity content. Many of the difficulties that arise stem from the anisotropic nature of the room-temperature (α) phase of uranium. The majority of nuclear fuel elements are manufactured from machined and heat-treated bars of cast uranium metal. Powder metallurgy practices are not practical due to irregular sintering characteristics and the pyrophoric nature of fine uranium particles. As with other metals, the tensile properties of uranium can be improved

N.R. Gubel (✉)
Department of Metallurgical and Materials Engineering, Colorado School of Mines, 1500 Illinois Street, Golden, CO 80401, USA
e-mail: ngubel@mines.edu

K.H. Eckelmeyer
6 Valley View Court, Placitas, NM 87043, USA
e-mail: keckelmeyer@comcast.net

K.N. Johnson
University of Tennessee, 908 Trent Lane, Knoxville, TN 37922, USA
e-mail: knjohnson629@gmail.com

M.J. Jackson
Center for Advanced Manufacturing, Purdue University, West Lafayette, IN, USA
e-mail: jacksonmj04@yahoo.com

J.S. Morrell
Y-12 National Security Complex, 1 Bear Creek Road, MS #8097, Oak Ridge, TN 37831, USA
e-mail: morrelljs@y12.doe.gov

J.S. Morrell and M.J. Jackson (eds.), *Uranium Processing and Properties*,
DOI 10.1007/978-1-4614-7591-0_1,

with alloying additions although options are inhibited by the low solubility of other elements in uranium. The study of uranium processing is an ongoing effort due to the inherent issues present in nuclear reactors used for electricity production; nuclear weapon production and dismantlement; the treatment, recycling, and storage of nuclear waste; and the cleanup of Cold War nuclear material production sites. These are causes of acute global interest, in all of which uranium is intimately involved.

Keywords Uranium metallurgy • Uranium alloys • Uranium metal • Mechanical properties • Microstructure • Martensite • Corrosion • Uranium oxide • Uranium hydride • Oxidation • Uranium decay • Uranium production • Stress corrosion cracking

1.1 Introduction

Uranium is found in modest concentrations in a wide variety of rocks, soils, and salt water. Approximately 0.0004 % of the earth's crust consists of naturally occurring uranium. This makes uranium about 1/20th as abundant as the common metals copper and nickel, approximately equally abundant as tantalum, and nearly 1,000 times more abundant than gold.

Several isotopes are present in naturally occurring uranium, as shown in Table 1.1. Of these, U^{238} strongly predominates at 99.27 %, followed by U^{235} at only 0.72 %. Both U^{238} and U^{235} are mildly radioactive, with half-lives of 10^9 and 10^8 years, respectively. The levels and types of radioactivity given off are relatively mild and non-penetrating, making external exposure to bulk uranium fairly safe. Inhalation or ingestion of finely divided uranium is more dangerous due to a combination of radioactivity and chemical toxicity. In general, uranium and lead are considered to be roughly comparable health hazards.

U^{235} is notable because it is fissionable by slow neutrons. Each fission event gives off a large amount of energy, as well as additional neutrons. The release of additional neutrons creates the possibility of self-sustaining chain reaction fission, thus providing the basis for the atomic bomb (where the chain reaction occurs in an uncontrolled fashion, releasing a huge amount of energy over a very short time), and nuclear power generation (where the chain reaction is carefully regulated and energy is released in a controlled manner, heating water to drive the turbines that power electrical generators). U^{238}, on the other hand, is only fissionable by very

Table 1.1 Naturally occurring uranium isotopes[a]

Mass	Percentage	Half-life (years)
238	99.27	10^9
235[b]	0.72	10^8
234	0.006	10^5

[a]Approximately 0.0004 % of earth's crust (~1,000 times more plentiful than gold)
[b]Fissions with slow neutrons

high energy neutrons. Because of this, U^{235} is the "high-equity isotope" for which uranium is mined and processed.

Isotopic separation is carried out by a number of processes. Magnetic separation (based on the same principle as mass spectroscopy) was used in the early 1940s, but has been abandoned in favor of gaseous diffusion and centrifugal separation which are faster and more efficient processes. Laser isotope separation was investigated more recently, and it is being developed as a production capability. All of the common separation techniques are based on very small differences between U^{235} and U^{238}, so they require a long cascade of low-efficiency individual separation steps. The product of the isotopic separation process is enriched uranium, and the by-product (depleted uranium) contains ~0.2 % U^{235} (i.e., ~99.8 % U^{238}).

1.2 Uranium Production

Uranium ores vary in chemical complexity from the relatively simple pitchblende ores, which are accompanied by perhaps ten other minerals, to extraordinarily complex uranium-bearing titanites, niobates, and tantalates containing rare earths and many other metallic elements.

Some pitchblende ore compounds may have in excess of 40 elements present from which uranium must be isolated. Most uranium deposits vary in composition, resulting in a constant variation in the composition of the starting materials. Such variations tend to be minimized by stockpiling methods. Because of this fact there have been many ad hoc procedures incorporated to meet special chemical situations all over the world. Highly specialized methods have no place in this publication. General features common to most extraction procedures will, however, be relevant. All common methods will include the following steps: (1) pre-concentration of the ore; (2) roasting or calcination to remove clays and carbonaceous materials, e.g., to increase solubility and improve the extraction; (3) a leaching operation to convert the uranium into an aqueous form; and (4) recovery of the uranium from the loaded leach liquors by ion exchange, direct precipitation, or solvent extraction. A brief summary of some special methods used for recovery of by-product uranium is mentioned toward the end of this section. The product of these operations is a high-grade concentrate, which is usually further purified at a site other than the uranium mill.

The element uranium is strongly electropositive, resembling aluminum and magnesium in this respect; consequently uranium metal cannot be prepared by reduction with hydrogen. Uranium metal has been prepared in a number of ways: reduction of uranium oxide with strongly electropositive elements, such as calcium, electrodeposition from molten salt baths (direct electrolytic reduction), thermal decomposition, decomposition of uranium halides (van Arkel de Boer "hot wire" method), and reduction of uranium halides (UCl_3, UCl_4, UF_4) with electropositive metals (Li, Na, Mg, Ca, Ba) [1]. Uranium metal is manufactured by the metallothermic reduction of uranium tetrafluoride (UF_4, often called green salt)

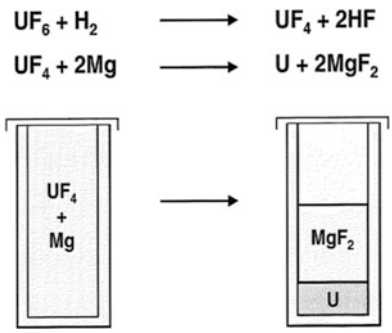

Fig. 1.1 UF_4 reduction process

with a reactive metal, usually magnesium. The enriched or the depleted UF_6 product of the isotopic separation process can either be converted to oxide (enriched oxide pellets for assembly into nuclear fuel rods) or reduced to metallic uranium, as illustrated in Fig. 1.1. The initial reduction step involves reaction of UF_6 with hydrogen to form UF_4. The UF_4 is then reduced to metallic uranium by elevated temperature reaction with magnesium or other alkali or alkaline earth metals. This produces liquid uranium covered with a blanket of MgF_2 slag. After the reaction has gone to completion the reaction vessel cools and the uranium and slag solidify. Typical production runs produce anywhere from approximately 4 kg to greater than 50 kg of metal product in the form of a fused button depending on enrichment levels.

The resulting uranium "derbies" are removed and cleaned. Casting is done in vacuum-induction furnaces using graphite molds and crucibles. The molds are coated with a thin ceramic layer (typically rare-earth oxide) to minimize the carbon contamination of the cast products. They can then be vacuum remelted, cast into shapes of interest, or formed by a variety of standard metal working processes. Alloying elements are sometimes added during the remelting process for purposes to be discussed later. Large-scale production of uranium metal requires elevated temperature where the high reactivity of uranium with most common refractory materials and metals makes the selection of container vessels a difficult problem.

Uranium metal can be melted and fabricated using the same methods that are employed with most other metals. It can be hot worked by processes such as rolling, forging, and extrusion; cold worked by rolling, swaging, or a variety of sheet metal forming processes; and welded and machined by most standard methods. It is very prone to oxidation, however, so melting, welding, and heat treating are usually done in inert environments or in vacuum. Similarly, finely divided uranium is pyrophoric, requiring special precautions to be taken in machining. The hazards associated with ingestion or inhalation also require special precautions to be taken in work areas where finely divided uranium metal or oxides are likely to be present.

Enriched uranium metal is used primarily for nuclear weapon and energy applications. Depleted uranium (DU) is used for applications requiring very high density, such as counterweights, shields, and kinetic energy penetrators (antitank rounds).

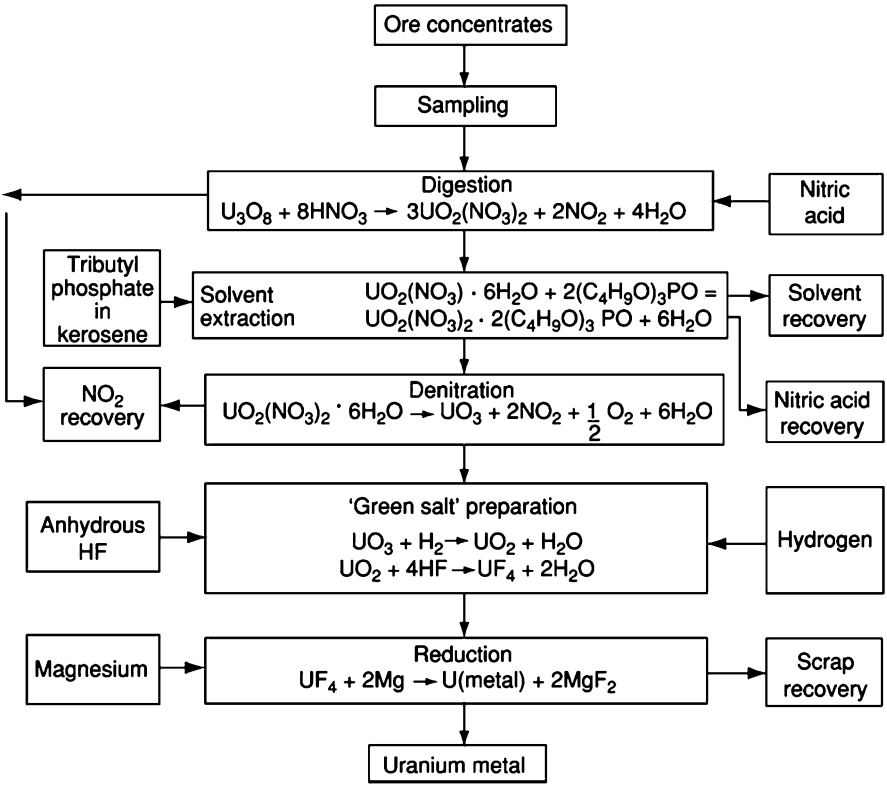

Fig. 1.2 Flow sheet for the production of uranium metal by reduction of UF_4 with magnesium [1]

The density of unalloyed uranium is 19.1 g/cm^3. This is more than twice the density of steel, and 68 % denser than lead. Among ductile materials, only a few precious metals, such as gold and platinum, exhibit comparably high densities. Tungsten is similar in density to uranium, but is brittle in elemental form. Tungsten powders are frequently liquid phase sintered with ductile metal binders. The resulting "tungsten heavy metal" composites have somewhat lower densities, but more useful engineering properties, and compete with DU for kinetic energy penetrator applications.

Chemical recovery of by-product uranium is necessary for both economic reasons and to maintain uranium in a suitable form. The major contributor to the waste stream is uranium metal fabrication operations that generate uranium scrap. This involves the casting, machining, rolling, and forming operations.

The chemical recovery system involves treatment of the low-equity scrap (Fig. 1.2), and it is generally derived from combustible materials (that are subsequently converted to contaminated uranyl nitrate solutions by means of several unit operations including dissolution, acidification, and evaporation). The low-equity scrap is typically processed for enriched uranium and consists of finely divided and highly oxidized scrap (machine turnings or skull material from castings).

The uranyl nitrate produced from low-equity scrap is purified in one or two stages depending on the setup. If two stages are used, the first is called primary extraction and uses dibutyl carbitol or other organics as the extraction agent. Dibutyl carbitol will extract nearly all of the enriched uranium from the process stream, but will also extract some contaminants. The raffinate from the primary extraction typically has a minimum level of uranium and can be sent directly to waste treatment. The second stage, known as the secondary extraction system, uses tri-butyl phosphate in kerosene as the extracting agent. The tri-butyl phosphate is highly selective toward uranium and rejects almost all contaminants, but leads to significant uranium losses in the raffinate that must be recycled back to primary extraction.

High-equity scrap generally consists of uranium oxide generated in the skull of the casting operations. The skull oxide is dissolved in nitric acid and sent directly to secondary extraction. The product leaving secondary extraction is evaporated to high-purity molten uranyl nitrate. The molten uranyl nitrate is heated to a trough-type de-nitrator and thermally decomposed to uranium trioxide. The uranium trioxide is transferred to the oxide conversion facility that consists of two fluidized beds. The first bed converts the uranium trioxide to uranium dioxide with hydrogen gas. The second fluid bed converts the uranium dioxide to UF_4 with anhydrous hydrogen fluoride gas. The green salt is subsequently reduced to uranium metal by a reactive metal. The product is a high-purity uranium button. The by-product is a slag consisting primarily of contaminated magnesium fluoride. This by-product is crushed, calcined, and dissolved in acidified aluminum nitrate solution and processed through primary extraction.

1.3 Electronic Structure of Uranium

The actinide series of elements has a complex electronic relationship wherein the 5f, 6d, 7s, and 7p orbitals are all at relatively comparable energies and electron shifting from the 5f to 6d can occur spontaneously. The electronic orbitals also overlap spatially, implying that actinide bonding can involve any or all of them. Regularly determining whether the complex bonding is covalent or ionic is impossible.

Differing from lanthanide chemistry is the contribution of covalent-hybrid bonding involving the 5f electrons. Relative to the 5s and 5p orbitals, the 5f orbitals have a much greater spatial extension relative to the 6s and 6p orbitals than that of the 4f to the 5s and 5p orbitals. Hybrid bonding has all been shown experimentally, most often involving the 5f overlap with fluorine ions and the covalent-ionic bonding that occurs to form UF_3 and UF_6 compounds [2].

Uranium is very chemically reactive and bonds directly with most elements. Given the reactiveness of uranium, combined with the overlap of electronic bonding modes, a wide range of intermetallic compounds are formed while extensive solid solutions are unusual. Without delving into further detail, the knowledge of

this situation that occurs with uranium and other actinides sheds light into the complexity of uranium kinetics and compatibility studies.

1.4 Uranium Metallurgy

The light actinide metals (Th–Pu) have always occupied unique placement in the periodic table because of their wandering 5f electrons and intricate crystallographic phases at high pressures and high temperatures [2]. The contributions of 5f electrons to bonding give rise to low-symmetry crystal structures and a narrow 5f-band related to the Fermi-energy level.

Uranium metal has been the subject of intense experimental and theoretical investigation. Its crystallography and properties have been characterized to pressures as high as 100 GPa and temperatures up to 4,500 K. Solid uranium exhibits three polymorphic forms: gamma-phase (body-centered cubic (BCC)) above 775 °C, beta-phase (body-centered tetragonal) between 668 and 775 °C, and alpha-phase (orthorhombic) below 668 °C (see Table 1.2). The mechanical properties of these three phases are described in Table 1.3 of the following section. Gamma-phase is soft and ductile, whereas beta-phase is brittle. The properties of alpha-phase vary substantially with temperature, as will be discussed in more detail.

Table 1.2 Allotropes of uranium including ranges of temperature stability and lattice arrangements

Allotrope	Temperature range of stability (°C)	Space lattice and space group	Unit cell dimensions (Å)	Atoms per unit cell
α	<668	Orthorhombic	$a = 2.854$, $b = 5.865$, $c = 4.955$	4
β	668–775	Tetragonal P42 nm or P42 mnm	$a = 5.656$, $b = c = 10.76$	30
γ	775–1,130 °C (T_m)	Body-centered cubic	$a = 3.524$	2

Table 1.3 Uranium allotropes and respective standard mechanical properties

Allotrope	Structure	Temperature range (°C)	Mechanical behavior
		<200	Decreasing ductility, decreasing slip, increasing twinning, ductile-to-brittle transition
α	Orthorhombic	200–400	Ductile, deforms primarily by slip, strain hardens, does not recrystallize
		>400	Soft and ductile, deforms readily by slip, dynamically recrystallizes
β	Tetragonal	668–775	Brittle
γ	Body-centered cubic	764–1,130	Soft and ductile, deforms readily by slip, dynamically recrystallizes

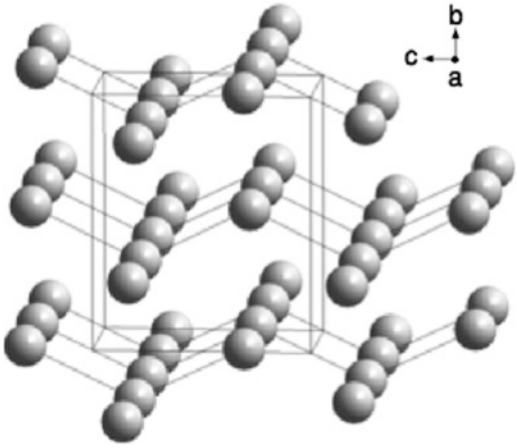

Fig. 1.3 The structure of α-uranium is a layered structure with *ac*-layers perpendicular to the *b*-axis with clear strongly bonded and corrugated (010) planes. The uranium–uranium distances in the ac layer are (2.80 ± 0.05) Å and between the layers 3.26 Å [1]

The α-structure consists of corrugated sheets of atoms, parallel to the *ac*-plane and perpendicular to the *b*-axis. Within the sheets the atoms are tightly bonded, whereas the forces between atoms in adjacent sheets are relatively much weaker (Fig. 1.3). This arrangement is highly anisotropic and resembles the layer structures of arsenic, antimony, and bismuth.

Both the interstitial sites in α- and β-U phases are too small to be occupied by interstitials. These facts are in agreement with the lack of primary solid solubility of the interstitial impurity atoms carbon, nitrogen, and oxygen in the α- and β-U phases and the very limited substitution solid solubility of certain transition metals in β-U [3]. The limited solubility tends to invoke complex formation; if suitable complexes exist, these could provide interstitial positions for the 3d impurity atoms such as iron, manganese, nickel, and cobalt in the α- and β-U phases. Because of strong U–M bonding both in α-U and β-U, the presence of solute atoms M will transform the geometry of their neighboring uranium atoms into complexes which lead to anisotropy.

The physical properties of the α-phase are a reflection of its structure, e.g., the strongly anisotropic coefficient of thermal expansion. The large anisotropy is obvious at room temperature and increases with temperature [4]. The average values of the thermal expansion coefficient over the temperature range 25–325 °C are 26.5, −2.4, and 23.9×10^{-6}, respectively, along *a*, *b*, and *c*. A chemical consequence of the unique orthorhombic structure of α-uranium is that the formation of solid solutions with metals of the common structure types is severely restricted [1, 5].

The β-phase of uranium exists between 668 and 775 °C; it has a complex structure with six crystallographically independent atoms in the tetragonal unit cell [6]. The space group is P42/mnm, P42nm, or P4n2, with unit cell parameters $a = 5.656$ Å and $b = c = 10.759$ Å. The tetragonal lattice is a stacked layer structure with layers parallel to the *ab* plane of the unit cell at c/4, c/2, and 3c/4.

Additional high-precision measurements are required to solve the structure completely [1, 6].

The γ-phase of uranium is formed at temperatures above 775 °C; it has a BCC structure with the cell parameter $a = 3.524$ Å. The gamma-phase can be stabilized to room temperature by moderate alloying additions, for example 10 wt% Mo, thus facilitating characterization of the gamma-phase in early studies.

1.4.1 Mechanical Properties of Unalloyed Uranium

Alpha-uranium might best be described as a hybrid between a metal and a covalently bonded solid. In face-centered cubic metals each atom is surrounded by 12 equidistant nearest neighbors. This represents the arrangement in which "spherical atoms" can be most closely packed, and is most suggestive of nondirectional "central force field bonding" associated with "ideal metallic behavior."

Accordingly, FCC metals (such as aluminum and copper) are typically ductile at all temperatures and exhibit very low electrical resistivity. In BCC metals, on the other hand, bonding is somewhat more directional, indicating less ideal metallic behavior. Each atom is surrounded by eight nearest neighbors, and then four next-nearest neighbors at somewhat greater distances. Comparing FCC and BCC iron, it can be seen that the eight-nearest neighbors are actually somewhat closer in the BCC arrangement than in FCC, while the four next-nearest neighbors are considerably more distant. The "less ideal metallic bonding" characteristic of BCC metals (such as iron and many of the refractory metals) typically results in higher strength, a ductile-to-brittle transition at lower temperatures, and somewhat higher electrical resistivity. Contrary to the situation with titanium and zirconium, the introduction of small amounts of oxygen or nitrogen does not have an adverse effect on the mechanical properties of the metal.

Alpha-uranium takes this progression one step further. In alpha-uranium the atoms are arranged such that each atom has neighbors at four different distances. Four atoms are even closer than in BCC gamma uranium, whereas eight are farther away. As mentioned previously, the most closely spaced atoms are arranged in "tightly bonded" corrugated planes, with relatively large separations characteristic of much "weaker bonds" between adjacent corrugated planes, as illustrated in Fig. 1.3. This is indicative of a greater component of directional covalent bonding, rather than ideal metallic bonding. Consistent with this, alpha-uranium exhibits still higher electrical resistivity than BCC metals. Alpha-uranium also exhibits relatively high strength and brittle behavior at low temperatures. Fortunately, however, the ductile-to-brittle transition in alpha-uranium is slightly below room temperature, making it a useful engineering material.

The mechanical properties of alpha-uranium vary substantially with temperature, as shown in Fig. 1.4. The tightly bonded corrugated basal planes in alpha-uranium result in a very limited number of slip systems. In fact, room-temperature slip occurs only on these corrugated basal planes parallel to the direction of the

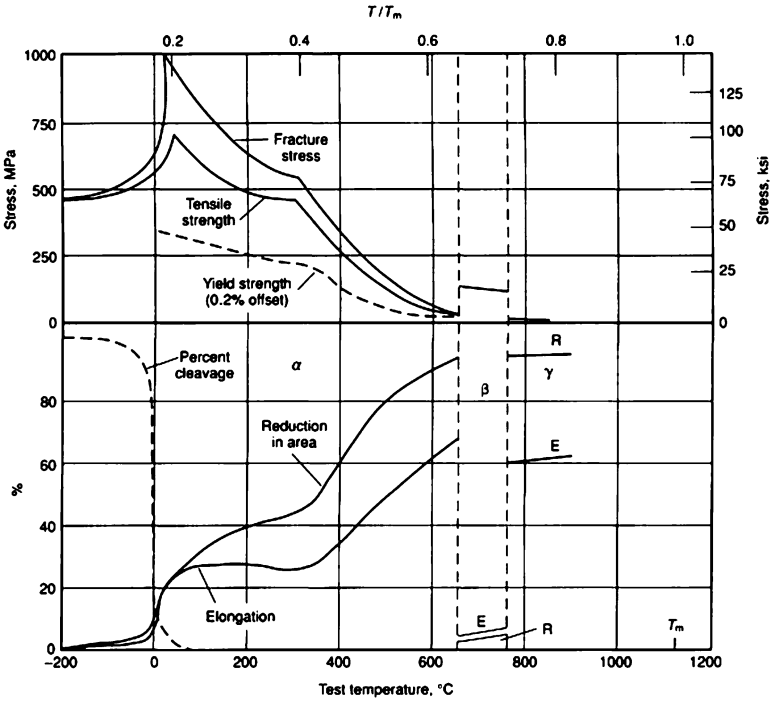

Fig. 1.4 Effect of temperature on the tensile properties of unalloyed uranium [7]

corrugations (the (010)[100] system). This singular slip system would not support macroscopic ductility were it not supplemented by a multiplicity of twinning systems. Combined, however, these provide a modest level of room-temperature ductility.

As temperature increases to ~250 °C and above, additional slip systems become active and the material becomes softer and much more ductile. Hence, while uranium plates can be cold rolled, warm rolling in the 250–350 °C range is much easier. Material that is warm rolled in this temperature range retains elongated grains and substantial work hardening. Previously cold or warm worked plates are sometimes recrystallized at 500–600 °C, but frequently the material is left in the worked condition, as will be discussed later.

Dynamic recrystallization begins in the vicinity of 400 °C, but varies substantially with rolling temperature and reduction, as well as the purity of the material. Ingots are typically heated to ~630 °C in molten salt in preparation for hot rolling. The molten salt prevents excessive surface oxidation, as would occur if the material were heated to this temperature in air. Substantial reductions are possible before the temperature drops below the dynamic recrystallization temperature. Plates are typically reheated in salt if additional amounts of hot working are needed.

Table 1.4 Room-temperature tensile properties of annealed uranium

Form	Heat treatment	YS (MPa)	UTS (MPa)	Elong (%)
Cast	None	200	450	6
Cast	Hydrogen outgassed at 630 °C	185	560	13
Cast	Hydrogen outgassed and beta grain refined at 720 °C	295	700	22
600 °C rolled	Preheated in salt (no hydrogen outgassing)	270	575	12
600 °C rolled	Hydrogen outgassed at 630 °C	270	720	31
600 °C rolled 300 °C finished	Hydrogen outgassed at 630 °C and 550 °C (final)	220	750	49

At temperatures below ~0 °C slip becomes more difficult, even on the preferred (010)[100] system. A transition from ductile to brittle behavior accompanies this decrease in slip and increase in twinning. As in steel, the ductile-to-brittle transition temperature is strongly influenced by microstructure and impurities. Grain refinement suppresses the transition temperature; hence fine-grained wrought materials typically exhibit much better room-temperature ductility than coarse-grained castings. The presence of even small amounts (<1 ppm by weight) of dissolved hydrogen increases the transition temperature, thus decreasing room-temperature ductility. Preheating in molten salt typically introduces hydrogen, so subsequent vacuum outgassing (at 350–630 °C) is often employed to reduce hydrogen content, thereby enhancing room-temperature ductility. Warm working makes the material more tolerant of hydrogen (apparently by providing dislocation hydrogen sinks), thus suppressing the transition temperature and enhancing room-temperature ductility.

Table 1.4 shows typical room-temperature tensile properties of annealed uranium following various types of processing. As-cast material typically exhibits very large grains and contains 1–2 ppm hydrogen. These result in nonuniform deformation and low tensile ductility. Castings are often beta heat treated to refine the alpha grain structure and increase ductility, particularly if these treatments are done in vacuum to also reduce hydrogen content. Alpha-worked and recrystallized uranium contains much finer grains and exhibits substantially higher ductility, particularly when residual hydrogen has been removed by vacuum outgassing. Plates that have been extensively warm rolled exhibit yield and ultimate strengths as high as 650 and 1,200 MPa, respectively [8]. Elongations of 15–20 % can be retained at these warm-worked strength levels, even without hydrogen outgassing. Recrystallization of these previously warm-worked materials actually reduces both strength and ductility unless hydrogen is also removed during the recrystallization anneal.

While unalloyed uranium exhibits yield and ultimate strengths similar to those of mild steel, uranium is substantially less tough. In particular, uranium and uranium alloys exhibit relatively low toughness in tests using notched or pre-cracked samples. There is some indication that this is due to the triaxial stresses in such samples shifting the ductile-to-brittle transition to higher temperatures. In any event, room-temperature Charpy V-notch energies for unalloyed uranium

are typically in the 10–25 J range, whereas 20 J is often considered a bare minimum for structural steels. Uranium alloys heat treated to 950 MPa yield strength have a KIC value in the vicinity of 40 MPa $m^{1/2}$, considerably lower than high-strength steels at equivalent strength levels.

1.5 Uranium Alloy Metallurgy

Relatively few elements are metallurgically similar to uranium. Many exhibit liquid-phase immiscibility. Others are soluble in liquid uranium, but form only intermetallic compounds on solidification. Only a few exhibit substantial solid solubility at high temperature: Cr, Mo, Nb, Pu, Re, Rh, Ti, V, and Zr. All of these but Cr, Nb, and V form intermetallic compounds with uranium.

Uranium is often alloyed to improve its very limited resistance to oxidation and corrosion, as well as to increase its strength. As shown in Table 1.5, alloying additions such as titanium, niobium, molybdenum, zirconium, and vanadium are extensively soluble in the high-temperature gamma-phase, much less soluble in the intermediate-temperature beta-phase, and essentially insoluble in the low-temperature alpha-phase. Typical phase diagrams are shown in Fig. 1.5.

Table 1.5 Alloying elements solubility at high temperatures [9]

Phase/structure	Elemental solubility
α (Orthorhombic)	<0.3 %: all
β (Tetragonal)	<1 %: all
γ (BCC)	20–100 %: Mo, Nb, Ti, Zr 2–10 %: Au, Cr, Pd, Pt, Re, Rh, Ru, V

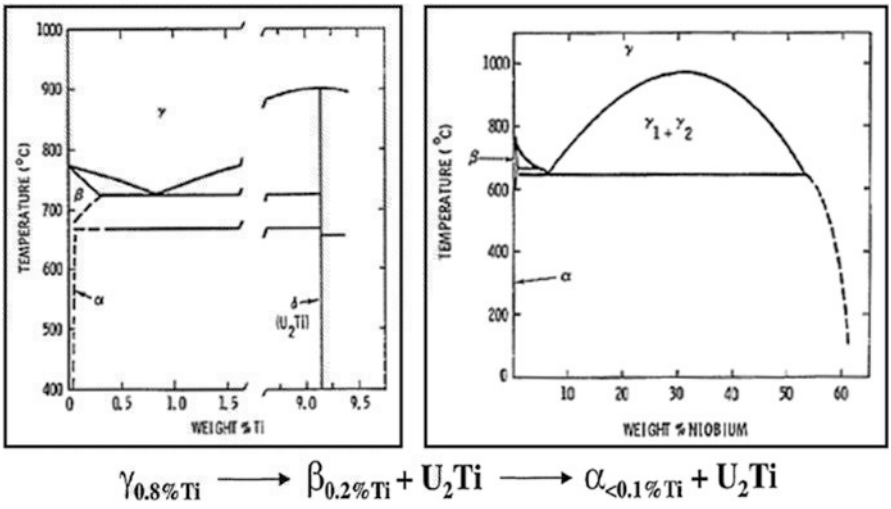

Fig. 1.5 Phase diagrams of uranium with decomposition of gamma-phase [10, 11]

	YS (MPa)	UTS (MPa)	Elong (%)
Unalloyed	220 – 270	575 - 720	12 - 30
U-0.8%Ti	520	1070	10

Fig. 1.6 Slow cooling results in diffusional transformations to two-phase microstructures. Brightfield micrograph of U-0.75Ti cooled from 800 °C at <1 °C/s showing light-etching acicular martensite and darker etching α + U_2Ti produced by the γ → α + U_2Ti reaction in the interstices between the martensite plates. Shown at 100× [9]

Titanium is most commonly used to increase strength, niobium and molybdenum to increase oxidation and corrosion resistance, and vanadium to refine alpha grain size in castings. Silicon, iron, and carbon are commonly present in concentrations of a few tens to a few hundreds of ppm, but are usually considered impurities, rather than deliberate alloying additions.

Uranium alloys are typically vacuum solution heat treated in the gamma range (~800–850 °C) to dissolve the alloying elements and remove hydrogen. The cooling rate from the solution treatment temperature is a critical parameter that determines subsequent microstructures and properties.

Slow cooling enables the gamma-phase to undergo diffusional decomposition, as described in Fig. 1.6. Hence, slowly cooled alloys typically exhibit two-phase microstructures in which the alloying elements are concentrated in the second phases, leaving the alpha-phase virtually devoid of alloying. The presence of the harder second phases results in modest increases in strength and decreases in ductility. However, oxidation and corrosion resistance remain similar to unalloyed uranium because the alloying elements are not retained in solid solution in the alpha-phase.

Figure 1.7 shows how quenching enables diffusional decomposition of the gamma-phase to be suppressed, thereby producing a variety of metastable microstructures that are supersaturated with alloying elements and exhibit a wide range of useful properties. Figure 1.8 summarizes the changes in microstructure, crystal structure, and strength that occur with increasing alloy content, regardless of whether alloying is done with titanium, niobium, molybdenum, or zirconium. However, the concentrations corresponding to the various transitions vary somewhat for different alloying elements.

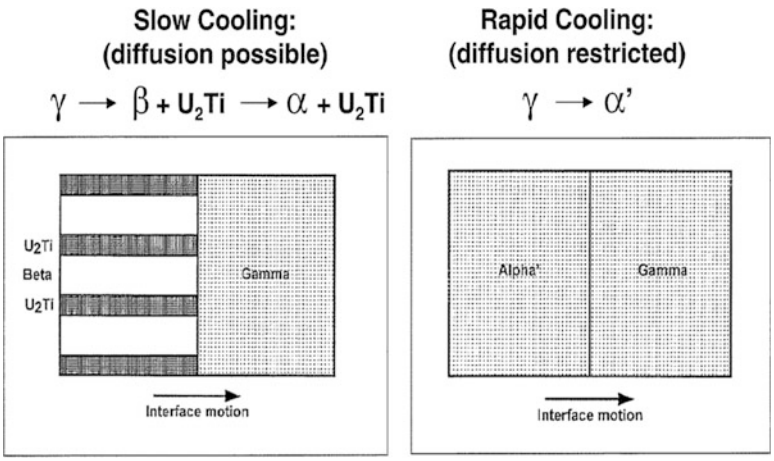

Fig. 1.7 Quenching effects on diffusion that promote martensitic transformation

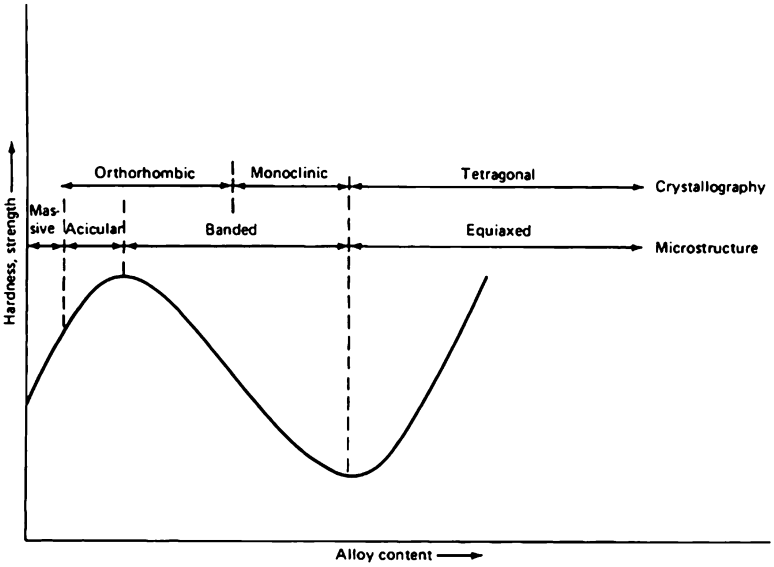

Fig. 1.8 Alloy content influencing microstructure, crystal structure, and properties [9]

Very dilute alloys (<0.3 wt% alloying addition) typically undergo the equilibrium sequence of phase changes on quenching from the gamma-phase. However, the combined rapid cooling 50 % and alloying additions enable the transformations to be suppressed to lower temperatures. This is sometimes exploited by using small vanadium additions to reduce alpha grain size in castings, as illustrated in Fig. 1.9.

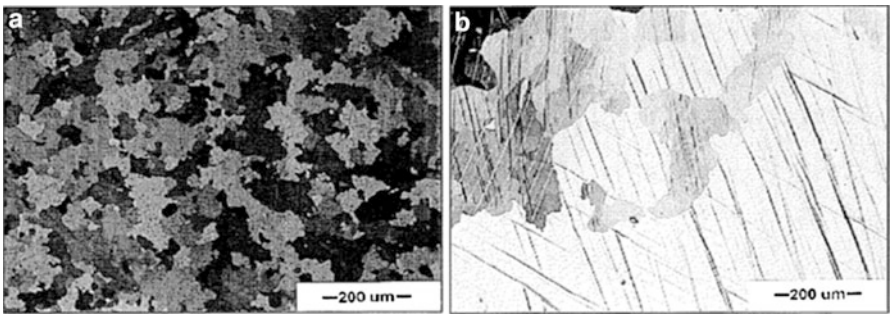

Fig. 1.9 Transformation of very dilute alloys at low temperatures. (**a**) U-0.27 %V, (**b**) unalloyed uranium. This transformation can be exploited to refine grain size in castings

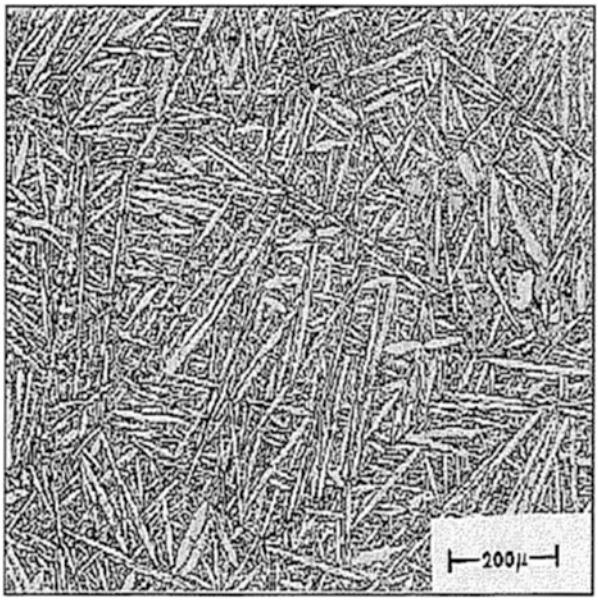

Fig. 1.10 Acicular martensite in U-0.8 % Ti rapidly quenched from 800 °C

In more concentrated alloys the equilibrium phase changes can be completely avoided by quenching. This results in a variety of supersaturated solid solutions being retained at room temperature. In alloys of intermediate concentration the gamma-phase transforms martensitically to one of several supersaturated variants of the alpha-phase. These are analogous to the low-carbon martensite in as-quenched maraging steel.

Quenched alloys containing approximately 0.5–1.5 wt% alloying addition undergo diffusion-less martensitic transformation to acicular martensite, as shown in Fig. 1.10. The alloy atoms retained in solid solution provide a substantial

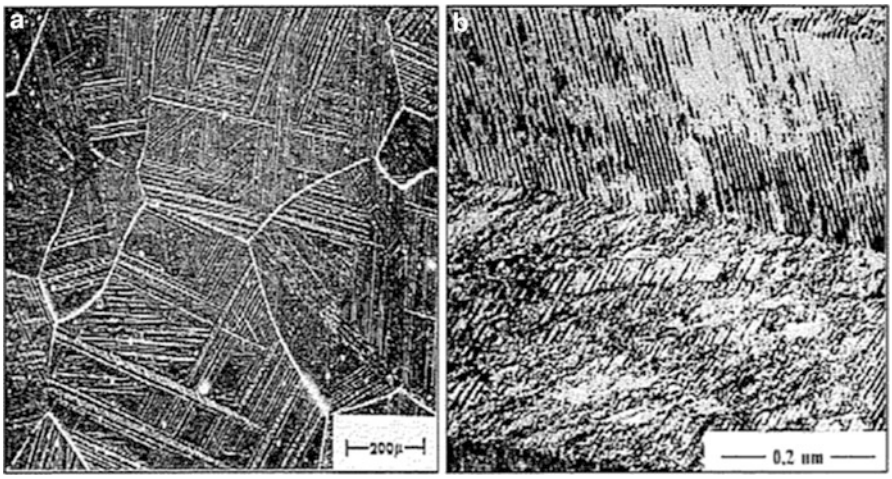

Fig. 1.11 Intermediate concentrations creating martinisitc twin-related parallel plates. (**a**) U-6 % Nb observed with polarized light, (**b**) same sample observed with TEM [10]

component of solid solution strengthening that increases with increasing alloy concentration. Unlike iron–carbon martensite, where the carbon atoms occupy interstitial sites and cause dramatic increases in strength and decreases in ductility, the alloying atoms in uranium martensites occupy substitutional sites. As a result they cause more moderate strengthening and permit good ductility to be retained. For example, as-quenched U-0.75 % Ti has a yield strength of ~650 MPa, three times that of unalloyed uranium, but exhibits 30 % tensile elongation and 50 % reduction in area.

Quenched alloys containing somewhat higher alloy concentrations (for example, 2–6 wt% niobium) also transform martensitically, but the morphology of the martensite is substantially different. These martensites consist of packets of twin-related parallel plates. The individual plates also contain a profusion of internal twins. This microstructure is shown at low and high magnifications in Fig. 1.11. These are frequently termed "banded martensites" to distinguish them from the "acicular martensite" characteristic of lower alloy contents. Complicating matters still more, the lattice angle gradually departs from 90°, causing a slight crystal structure change from orthorhombic to monoclinic.

The morphology of the banded martensites is similar to thermoelastic martensites that was observed in a number of nonferrous systems. Initial plastic deformation in these structures occurs by twin reorientation, rather than slip. When stresses are applied, favorably oriented twin variants grow at the expense of unfavorably oriented ones, as illustrated in Fig. 1.12. The curious decrease in hardness and strength with increasing alloy content is apparently caused by increasing twin boundary mobility, although the details of this are not completely understood. As with other thermoelastic martensites, a shape memory effect occurs in banded uranium martensites, particularly those near the hardness minimum.

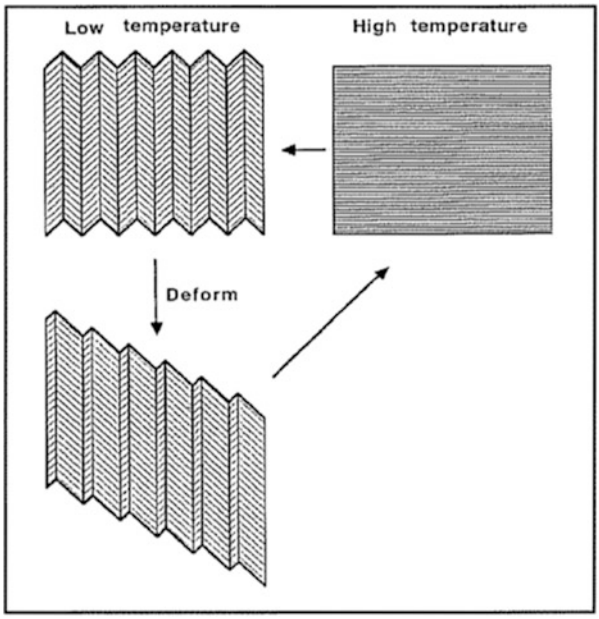

Fig. 1.12 Twin boundary mobility and shape-memory effect

The plastic deformation associated with twin reorientation (approximately 5 % tensile strain in U-6 % Nb) can be completely recovered by heating to the temperature at which the alpha-martensite reverse transforms to the parent phase (a variant of gamma-phase).

Alloys of still higher concentration (above ~6.5 wt% Nb or ~5.5 wt% Mo) retain metastable variants of the gamma-phase when quenched. The martensite start and finish temperatures decrease with increasing alloy content. If the M_s is suppressed to below room temperature, supersaturated variants of the gamma-phase are retained at room temperature. These are analogous to austenitic stainless steels. The primary microstructural features are typically the gamma-phase grain boundaries, as shown in Fig. 1.13. Under some conditions, however, parallel substructural features appear within the gamma grains. These correspond to domains within ordered variations of gamma-phase.

Alloys must be cooled at some critical rate or faster to avoid diffusional transformation and obtain these supersaturated structures, as illustrated in Fig. 1.14. The critical cooling rates vary with alloy content [12]. Relatively dilute alloys require rapid quenching. This restricts the section thicknesses in which they can be effectively heat treated. For example, cooling rates of ~100 °C/s or higher are required to obtain near-fully martensitic microstructures in U-0.75 wt% Ti—this limits the use of this alloy to section thicknesses of ~3 cm or less. Furthermore, increasing the alloy content in relatively dilute alloys actually increases quench rate sensitivity. This occurs because the M_s temperatures in dilute alloys are above the knee of the C-curve for diffusional decomposition (typically ~530 °C). The "critical quenching rate" in these alloys is defined by the intersection of the C-curve with the M_s. Increasing alloy content typically pushes the C-curve to longer

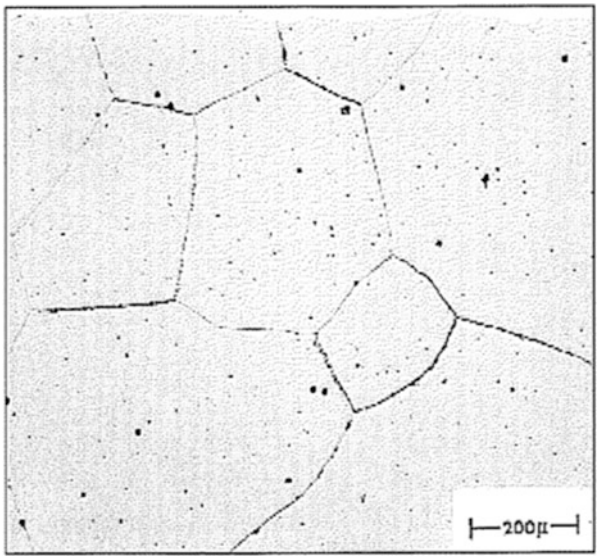

Fig. 1.13 Concentrated alloy consisting of U-10 % Mo showing the typical gamma-phase grain boundaries

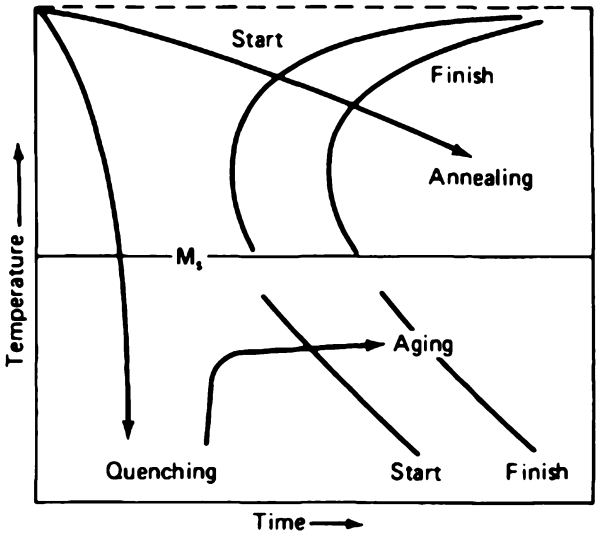

Fig. 1.14 Generalized time–temperature-transformation diagram showing heat treatments employed with uranium alloys. Increasing alloy content shifts diffusional transformations to longer times and decreases martensite transformation temperature. Quenching results in diffusion-less transformation of γ-phase to supersaturated martensites, which can be subsequently age hardened. M_s martensite start temperature [9]

times, but also lowers the M_s temperature. The decrease in M_s pushes the "critical intersection" to a lower temperature on the C-curve where diffusional decomposition occurs in shorter times. The net effect is that higher quenching rates are required to suppress diffusional decomposition prior to the onset of martensite formation, as shown for U-0.6 to 1.5 wt% Ti alloys in Fig. 1.15.

More concentrated alloys require less severe quenching, so they can be processed in thicker sections. For example, U-6 wt% Nb can be cooled at rates as low as ~10 °C/s and still get fully martensitic microstructures. U-10 wt% Mo is so quench-rate insensitive that it does not require artificial quenching—supersaturated

Dilute alloys
(Ms above knee of C-curve):
- Decrease in Ms dominates
- Critical quench rate increases

% Ti	Cooling Rate for 50% Martensite (°C/sec)
0.60	10
0.75	30
1.0	41
1.5	>45

Concentrated alloys
(Ms below knee of curve):
- Increased time for diffusional transformations dominates
- Critical quench rate decreases

%Nb	Cooling Rate for 100% Martensite (°C/sec)
2.3	>45
4.5	14
6.0	8

Fig. 1.15 Alloy content effects with dilute and concentrated alloys [10, 11]

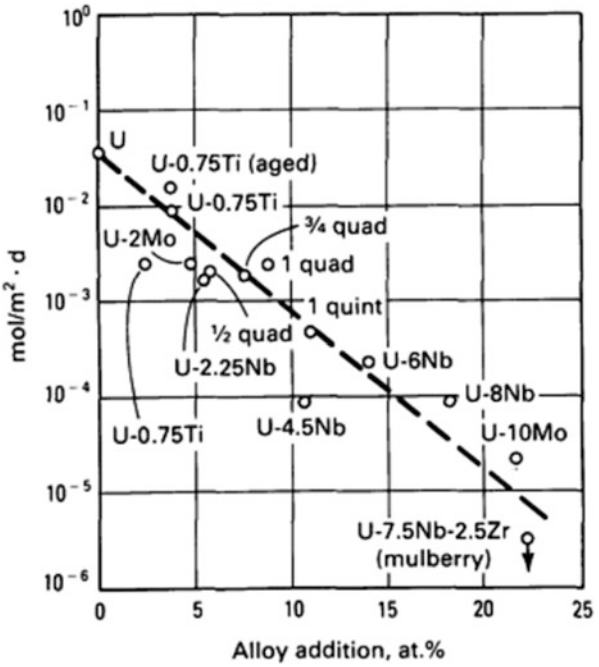

Fig. 1.16 Oxidation and corrosion resistance increase with alloying addition in solid solution for selected uranium alloys [13]

variants of the gamma-phase are retained even after air-cooling. Furthermore, once alloy content is sufficiently high to suppress the M_s temperature below the knee of the *C*-curve, the *C*-curve alone defines the critical quenching rate. As a result, further increases in alloy content now decrease quench rate sensitivity, as shown for U-2.3 to 6.0 wt% Nb alloys in Fig. 1.16. This is similar to the effect typically observed in alloy steels.